Space-Borne Multibeam Array Pattern Synthesis for Increasing Capacity

Haiwei Song[1, 2, *], Guang Liang[1, 2], Wenbin Gong[2], and Jinpei Yu[1, 2]

Abstract—The traditional pattern synthesis method of space-borne array is to achieve a "iso-flux" beam coverage via approximating a desired pattern; however, the synthesized pattern may not optimize the whole satellite communication (SatCom) system performance. This paper analyzes the interference in multibeam SatCom system using CDMA, and establishes the relation model between user capacity and multibeam pattern. Additionally, a novel particle swarm optimization (PSO) based on simulated annealing (SA) pattern synthesis method is proposed, which chooses user capacity as synthesis objective function. The numerical analysis, which is performed for a hexagonal array with 19 stacked patch elements, confirms that user capacity is at least doubled with the "max-gain-flux" beam coverage implemented by our method, compared to the "iso-flux" coverage when communication outage probability is 10%.

1. INTRODUCTION

In SatCom system, the contradiction between high gain and wide coverage of antenna can be resolved by space-borne multibeam array effectively, which has been a typical payload in global SatCom system [1, 2]. One of the key technologies in space-borne multibeam array antenna is the power pattern synthesis technology, which requires not only broad main-lobe beamwidth, but also low side-lobe level (SLL). It may be quite difficult for the classic analytic method, such as Dolph-Chebyshev, to achieve a satisfactory multibeam pattern, especially when the numerous elements are used.

Since genetic algorithm (GA) was applied to pattern synthesis by Johnson and Rahmat-Samii in 1994 [3], evolutionary algorithm has been widely used in the large-scale array pattern synthesis problem. 16 shaped beams were synthesized via real-code GA (RCGA) algorithm in space-borne hexagonal transmitter array with 61 elements [4, 5], and Recioui employed PSO to suppress SLL in linear array [6]. Recent advances in intelligent pattern synthesis focus on merging different kinds of intelligent algorithm, such as hybrid differential evolution (DE), and artificial bee colony (ABC) synthesis method has been applied to reconfigurable array synthesis [7]. Another trend in this field is the synthesis method based on convex optimization, which has remarkable global convergence properties and fast solving speed via interior-point algorithm. Wang et al. and Fuchs et al. proposed sequential convex optimization algorithm to implement arbitrary array pattern synthesis [8, 9].

However, a major problem of the above-mentioned synthesis method is considering only the array radiation performance improvement, no matter whether antenna pattern enhances the whole communication system performance or not. User capacity in multibeam SatCom system is a key performance metric, and almost no objective of space-borne array pattern synthesis method is to maximize the user capacity in the current SatCom system. Gilhousen et al. firstly analyzed the capacity of multibeam SatCom system using CDMA, but the analysis did not consider the inter-cell interference caused by side-lobe of beam pattern [10]. Fu et al. established a comprehensive capacity analysis model

* Corresponding author: Haiwei Song (shw.phd@hotmail.com).
[1] Shanghai Institute of Microsystem and Information Technology, Chinese Academy of Science, China. [2] Shanghai Engineering Center for Microsatellites, China.

of multibeam CDMA-based SatCom and showed the effect of imperfect power control; however, the basis of their analysis relied on a non-shaped tapered-aperture antenna pattern, such that the accuracy of capacity analysis would decline [11, 12]. In [13], seven-beam pattern with "iso-flux" coverage was synthesized by GA, which is performed for standard hexagonal array (SHA), and capacity was analyzed in the 7-beam CDMA-based SatCom system with the existence of power control error (PCE), but this study made no attempt to optimize beam pattern for capacity increase.

This paper focuses on the pattern synthesis of receiving SHA with 19 elements, which is aimed at increasing user capacity under the background of multibeam SatCom system using CDMA. The outline for this paper is listed below. Section 2 shows the gain pattern model of SHA, and then develops capacity analysis model in practical shaped 7-beam SatCom system using CDMA. In Section 3, on the basis of the initial multibeam pattern given by RCGA, SA-based PSO for increasing capacity pattern synthesis algorithm is described in detail. Section 4 provides the numerical simulation results. Finally, some meaningful conclusions are presented in Section 5.

2. SYSTEM DESCRIPTION

2.1. SHA Antenna Pattern and Seven-Beam Coverage

The geometry of receiving SHA antenna with 19 elements is depicted in Figure 1. Element space is 0.545λ, where λ is the wavelength of the L-band sinusoidal wave. The array response can be written as:

$$S(\theta, \varphi) = \sum_{i=1}^{19} I_i \exp\left\{jk_0(x_i u + y_i v) + \alpha_i\right\} F_i(\theta, \varphi) \tag{1}$$

where θ and φ are the elevation and azimuth angles in the spherical coordinate, and I_i and α_i are amplitude and phase excitation of element i in Figure 1. x_i and y_i are x- and y-coordinate positions of element i. $k_0 = 2\pi/\lambda$ is the wavenumber, and $u = \sin\theta\cos\varphi$, $v = \sin\theta\sin\varphi$. In (1), $F_i(\theta, \varphi)$ is the radiation pattern of individual element i, which is a dual-fed and dual-layer stacked patch antenna. Figure 2 shows three actual patterns of elements 2, 8 and 15 at $\varphi = 90°$, measured in spherical near-field anechoic chamber (Satimo) [14]. The normalized gain of SHA is given as follows:
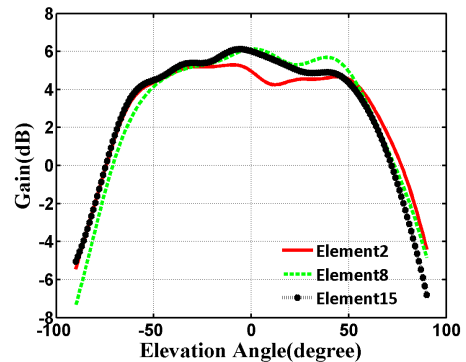
$$G = \eta \frac{|S(\theta, \varphi)|^2}{\frac{1}{4\pi} \int\limits_{0}^{\pi} \int\limits_{0}^{2\pi} |S(\theta, \varphi)|^2 \sin\theta d\theta d\varphi} \tag{2}$$

where $\eta \approx 0.9$ is radiation efficiency.

We employ the uplink seven-beam gain coverage mentioned in [13]. The ideal beam coverage is shown in Figure 3. The inner coverage contains center beam 1, whose half-power beamwidth (HPBW) of θ is required for greater than $\pm 20°$. Outer coverage has six beams, the θ-HPBW of beam 1/6/7 is
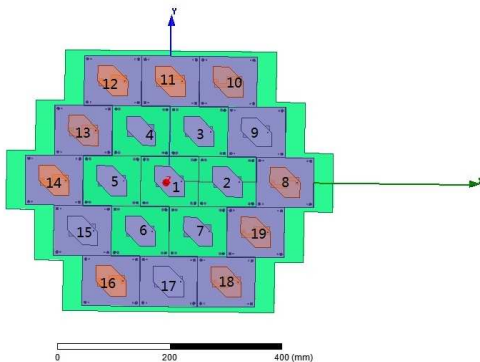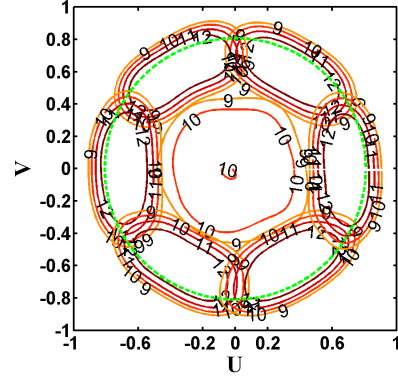

Figure 1. The geometry of SHA antenna.

Figure 2. Measured element pattern at $\varphi = 0°$.
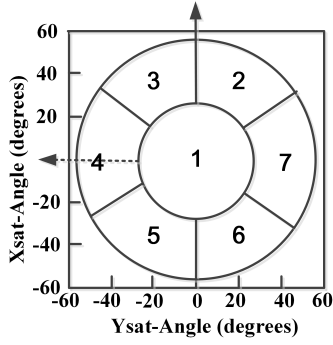
Figure 3. The desired seven-beam pattern coverage of receiving SHA antenna.

Figure 4. The contour of RCGA-based synthesis seven-beam pattern antenna.

$25° \sim 55°$, and the left beam's θ-HPBW is $-55° \sim -25°$. The desired seven-beam patterns are generated under the above requirements, and RCGA-based pattern synthesis method is adopted, which minimizes the mean-squared error between synthesized pattern and the desired pattern (discuss in Section 3). Figure 4 depicts the optimized seven-beam gain contours in uv space, and the dashed circle means the coverage requirement of $\pm 55°$.

2.2. The Interference Model of Seven-Beam CDMA-Based SatCom System

The interference of the desired user in the single satellite system using CDMA is from: a) the multiple access interference from other users in the same beam cell; b) interference from the users of adjacent beam in the same satellite; c) co-channel interference from other satellite systems. This paper does not take intra-system interference into account. It is assumed that users are distributed uniformly in all seven beams shown in Figure 3, and the user of interest is in the center beam. I_{S0} and I_{S1} represent the interferences of categories a) and b), respectively. The total interference I_S of user of interest is the sum of I_{S0} and I_{S1}.

Power control is employed to reduce the multiple-access interference in CDMA SatCom System, in order to improve user capacity. The round trip time (RTT) of LEO SatCom is greater than 10 ms, so open-loop power control is used generally [15]. If imperfect open power control is taken into account, I_{S0} is expressed as follows:

$$I_{S0} = \sum_{(j_0,k_0) \notin S0} \gamma_{jk} P_0 \tag{3}$$

where P_0 is the nominal user's terminal power into space-borne receiver with perfect power control. γ_{jk} is the kth user's open-loop PCE in the jth beam cell, and $(j_0, k_0) \notin S0$ means the user in center beam except the users of interest.

Beam cell is essentially formed via HPBW area of beam pattern. Due to the roll-off of main-lobe and SLL, multibeam cells are not absolutely separated. So, I_{S1} is written as follows:

$$I_{S1} = \sum_{(j,k) \in S1} \gamma_{jk} \beta_{jk}^2 P_0 \tag{4}$$

where $(j, k) \in S1$ means all the users in outer six-beams, and $2 \leq j \leq 7$. β_{jk}^2 is the antenna gain pattern discrimination factor, which is given as:

$$\beta_{jk}^2 = \frac{G_1(\theta_{jk}, \varphi_{jk})}{G_j(\theta_{jk}, \varphi_{jk})} \tag{5}$$

where $G_j(\theta_{jk}, \varphi_{jk})$ is the kth user's pattern gain of the jth cell, and the practical meaning is power compensation that keeps the same power in seven-beam coverage. $G_1(\theta_{jk}, \varphi_{jk})$ is the kth user's gain of

the center beam cell, which reflects the amount of the isolation between different beams. Formula (5) establishes an important relationship between the multibeam pattern and SatCom system, which is the basis of the following discussion.

2.3. Capacity Analysis

With the increase of users in SatCom system, the interference rises to the user of interest. When the desired user's bit energy-to-noise radio is below the threshold, the communication will be broken off. Wherefore, the outage probability of desired user is defined as:

$$P_{out} = \Pr\{EINR \le EINR_{req}\} \tag{6}$$

where $EINR$ can be expressed as:

$$EINR = \frac{B}{R_b} \times \frac{\gamma_0 P_0}{I + \eta} \tag{7}$$

where γ_0 is the PCE of the desired user, B the channel bandwidth, R_b the information bit rate, and η the noise power. After some simple transformations, the outage probability can be given by:

$$P_{out} = \Pr\left\{\frac{I_s}{P_0} \ge \frac{B}{R_b}\left[\frac{\gamma_0}{EINR_{req}} - \frac{1}{E_b/\eta_0}\right]\right\} \tag{8}$$

where η_0 is noise power spectral density, and $\eta_0 = kT_s$, where k is the Boltzmann constant and T_s the equivalent system noise temperature of SHA antenna. E_b/η_0 in Equation (8) can be written as:

$$\frac{E_b}{\eta_0} = \frac{P_0/R}{\eta/B} = \frac{P_t G_t G_r \lambda^2}{(4\pi d)^2 \times L_a \times R_b \times N_F \times k \times T_s} \tag{9}$$

where P_t and G_t are the transmitting power and antenna gain of the user terminal, respectively. G_r is the receiving gain of space-borne SHA antenna, d the distance between user terminal and satellite, L_a the axial ratio loss of SHA antenna, and N_F the noise figure of RF-front system.

The total normalized interference I_s/P_0 is expressed as:

$$\frac{I_s}{P_0} = \sum_{(j_0,k_0)\notin S0} \gamma_{jk} + \sum_{(j,k)\in S1} \gamma_{jk}\beta_{jk}^2 \tag{10}$$

where γ_{jk} is lognormal random variable [15], and $\gamma_{jk} = e^{\delta_{jk}}$, where δ_{jk} is a zero-mean Gaussian random variable in nepers. The mean and variance of I_s/P_0 are given by:

$$\mu_I = E\left[\frac{I_s}{P_0}\right] = g_1\left(N - 1 + \sum_{(j,k)\in S1}\beta_{jk}^2\right) \tag{11}$$

$$\sigma_I^2 = (g_2 - g_1^2)\left(N - 1 + \sum_{(j,k)\in S1}\beta_{jk}^2\right) \tag{12}$$

where g_1 and g_2 are shown as:

$$g_1 = \mathrm{E}[\gamma] = Ae^{h^2\sigma_s^2/2} + (1 - A)e^{h^2\sigma_{us}^2/2} \tag{13}$$

$$g_2 = \mathrm{E}[\gamma^2] = Ae^{2h^2\sigma_s^2} + (1 - A)e^{2h^2\sigma_{us}^2} \tag{14}$$

In (13) and (14), A is shadow probability factor, and A is usually 0.3 in LEO [18]. σ_s and σ_{us} are the standard deviations of PCE for shadowed users and unshadowed users in dBs, respectively. $h = \ln(10)/20$, which converts nepers into dBs.

When the desired user's PCE γ_0 is fixed, the conditional outage probability is:

$$P_{out}|\delta = \frac{1}{2}erfc\left(\frac{\varsigma - \mu_I}{\sqrt{2\sigma_I^2}}\right) \tag{15}$$

where ς is expressed as:

$$\varsigma = \frac{B}{R_b} \left[\frac{e^\delta}{EINR_{req}} - \frac{1}{E_b/\eta_0} \right] \tag{16}$$

because the desired user may be in shadowed or unshadowed state, the unconditional outage probability is given by:

$$P_{out} = A \int_{-\infty}^{\infty} P_{out}|\delta_s \cdot f(\delta_s)d\delta_s + (1 - A) \int_{-\infty}^{\infty} P_{out}|\delta_{us} \cdot f(\delta_{us})d\delta_{us} \tag{17}$$

where $f(\sigma_s)$ and $f(\sigma_{us})$ are the Gaussian distributions of σ for shadowed and unshadowed states, respectively. Formula (17) contains only one variable: user capacity N, which can be obtained when P_{out} is fixed.

3. PATTERN SYNTHESIS FOR INCREASING CAPACITY

3.1. Initial Element Excitations

The initial element excitation is acquired from RCGA-based pattern synthesis method, whose fitness function is conveyed as follows:

$$\min_{(I,\alpha)} \sum_{m=1}^{N_\theta} \sum_{n=1}^{N_\varphi} (G(\theta_m, \varphi_n) - G_d(\theta_m, \varphi_n))^2 \tag{18}$$

where N_θ and N_φ are the numbers of samples in the elevation plane and azimuth plane. $G_d(\theta_m, \varphi_n)$ is the desired beam pattern. $G_{d1}(\theta_m, \varphi_n)$ and $G_{d2}(\theta_m, \varphi_n)$ are the desired patterns of center beam and beam 2 and given by:

$$\begin{aligned} G_{d1}(\theta, \varphi) &= \begin{cases} 10.5\,\text{dB} & 0° \le \theta \le 35°, \ 0° \le \varphi \le 360° \\ 0\,\text{dB} & \text{others} \end{cases} \\ G_{d2}(\theta, \varphi) &= \begin{cases} 13\,\text{dB} & 36° \le \theta \le 60°, \ 30° \le \varphi \le 90° \\ 0\,\text{dB} & \text{others} \end{cases} \end{aligned} \tag{19}$$

The excitation of each element's amplitude and phase is selected as gene, and the float value of excitation is acted as gene encoding. The structure of this chromosome is defined as: $(I_1, I_2, \ldots, I_{19}, \alpha_1, \alpha_2, \ldots, \alpha_{19})$. The parameters of RCGA-based pattern synthesis are shown as follows: a) the population size is 200, and the maximum number of generations is 250. b) the generation gap factor is 0.96, and re-insect method is applied that can replace least-fit parents. c) intermediate crossover is used, and the crossover probability is 0.9. d) the mutation probability is 0.15.

3.2. Simulated Annealing-Based PSO Pattern Synthesis Algorithm

PSO is an effective population-based intelligence algorithm inspired by the social behavior of bird flocking or fish schooling. In PSO, each particle searches the best positions in multi-dimensional space according to its self-cognitive and social experience. Clerc and Kennedy proposed inertial weight and constriction factor to adjust the velocity of the particle for obtaining better convergence [16].

We select the chromosome defined in RCGA as the position vector in our PSO algorithm, and in the $(n + 1)$th iteration the position of ith particle is given by:

$$\mathbf{x}_i(n + 1) = \mathbf{x}_i(n) + \mathbf{v}_i(n + 1) \tag{20}$$

where $\mathbf{x}_i(n)$ is the position vector of nth iteration, and $\mathbf{v}_i(n + 1)$ is velocity vector in the $(n + 1)$th iteration, which determines the search direction and can be expressed as:

$$v_{ij}(n + 1) = \chi \left[v_{ij}(n) + c_1 r_{1j}(n) (p_{ij}(n) - x_{ij}(n)) + c_2 r_{2j}(n) (\tilde{p}_{gj}(n) - x_{ij}(n)) \right] \tag{21}$$

where $v_{ij}(n)$ is the dth component of velocity vector of ith particle, and $j = 1, 2, \ldots, 38$. c_1 and c_2 are cognitive and social parameters, respectively, and they are always positive constants, which control the impact of the local-best position $p_{ij}(n)$ and global-best position $\tilde{p}_{gj}(n)$. Both $r_{1j}(n)$ and

$r_{2j}(n)$ are random numbers distributed uniformly between 0 and 1. χ is constriction factor, and $\chi = 2/|2 - C - \sqrt{C^2 - 4C}|$, where $C = c_1 + c_2$, and the general requirements $C > 4$ can obtain better convergence.

Although constriction factor can improve the global convergence of PSO, the immature convergence problem cannot be avoided. A PSO based on SA pattern synthesis algorithm is applied in this paper. SA algorithm imitates the temperature falling process of heated solid, and it is a quite effective method to avoid trapping into local optimum [17]. The thoughts of the proposed algorithm is that $\tilde{p}_{gj}(n)$ in (21) is updated in probability under the control of SA. In this algorithm, the normalized receiving probability is calculated for every particle, which is expressed as follows:

$$P_i = \frac{e^{-(f_i - f_g)/T}}{\sum\limits_{i=1}^{N_p} e^{-(f_i - f_g)/T}} \tag{22}$$

where $f_i = f(\mathbf{x}_i(n))$, $f_g = f(\tilde{\mathbf{P}}_g(n))$. $T = T(n)$ is annealing temperature parameter, which decreases with increasing time. According to the receiving probability, the global best particle is selected by roulette wheel strategy, and the selection probability Pb_r is defined as:

$$Pb_r = \frac{P_r}{\sum\limits_{i=1}^{r} P_i} \tag{23}$$

where P_r is the receiving probability of the rth particle and p_{bet} a random number between 0 and 1. When $Pb_r \geq p_{bet}$, the position of rth particle is chosen as global best position in the current iteration.

Procedure: SA-based PSO for Increasing Capacity (SAPSOIC) pattern synthesis algorithm

Step 1:	*Set the number of particle N_p and the maximal iteration number M. Initialize the parameter c_1 and c_2, and the annealing constant λ_{SA}. Set the limit of user per beam $[N_l, N_u]$.*
Step 2:	*Set $\mathbf{x}_i(0) = \mathbf{w}(0) + \Delta\mathbf{w}_i$, where $\Delta\mathbf{w}_i = [\Delta\mathbf{I}^0_{1\times 19}, \Delta\alpha^0_{1\times 19}]^T$, $\Delta\mathbf{I}^0_{1\times 19}$ and $\Delta\alpha^0_{1\times 19}$ are randomized uniformly vector in $[-2, 2]$, and $[0, 2\pi]$, $i = 1, 2, \ldots, N_p$. $\mathbf{w}(0)$ is the initial excitations from RCGA.*
Step 3:	*for $m = N_l$ to N_u*
	Calculate P_{out}, set $f_i = P_{out}$, and evaluate $f_g = \min\{f_i, i = 1, 2, \ldots, N_p\}$, set the best position $\mathbf{p}_g$;
	Set the initial annealing temperature $T = -f_g/\ln(5)$;
	for $t = 1$ to M
	Evaluate receiving probability P_i of every particle;
	for $r = 1$ to N_p
	Evaluate every particle's selection probability Pb_r;
	$p_{bet} = rand(0, 1)$;
	if $p_{bet} \leq Pb_r$
	$p_g = x_r(t)$;
	break;
	end if
	end for
	Update the velocity vector $\mathbf{v}_i(n+1)$ and position vector $\mathbf{x}_i(n+1)$, $i = 1, 2, \ldots, N_p$;
	Evaluate the new fitness of every particle, and update $\mathbf{p}_g$ and $\mathbf{p}_i$, $i = 1, 2, \ldots, N_p$;
	Update $T = \lambda_{SA}T$;
	end for
	Randomize the new excitations $\Delta\mathbf{w}_i$, and set $\mathbf{x}_i(0) = \mathbf{p}_g + \Delta\mathbf{w}_i$, $i = 1, 2, \ldots, N_p$;
Step 4:	*end for*
end procedure	

Capacity N is given in terms of outage probability, and it is quite difficult to derive the analytic expression of capacity. However, outage probability is risen as capacity is increased, and if outage probability is minimized for a given capacity, then in the same requirements of outage probability, e.g., $P_{out} = 10\%$, communication system has more considerable user capacity. So, the optimized model of SA-based PSO pattern synthesis is given as:

$$\min_{I,\alpha} A \int_{-\infty}^{\infty} P_{out}|\delta_s \cdot f(\delta_s)d\delta_s + (1 - A) \int_{-\infty}^{\infty} P_{out}|\delta_{us} \cdot f(\delta_{us})d\delta_{us} \tag{24}$$
$$\text{s.t} \quad N = N_u$$

where N_u is the current user number per beam, which will be increased with the algorithm iterations. The pseudocode of SA-based PSO for Increasing Capacity (SAPSOIC) pattern synthesis algorithm is given.

4. NUMERICAL SIMULATION

The geometric formula is given in [13], which is about the distance r from user's position in beam coverage to the sub-satellite point and the elevation θ of SHA antenna, and the azimuth of user in beam is the same as φ of antenna. By randomizing r and φ repetitively, users are distributed uniformly in the overall beam coverage, and then the initial pattern gain of user is immediately obtained according to the excitations of RCGA synthesis. Finally, the initial outage probability can be calculated by means of Monte-Carlo method. In every iteration of our proposed algorithm, the fitness function, i.e., outage probability, is evaluated by repeating the same process mentioned above.

4.1. Input Parameter

The main SatCom system parameter is listed below: satellite orbit altitude $H = 900\,\text{km}$; bit rate $R_b = 9.6\,\text{kbps}$; channel bandwidth $B = 7\,\text{MHz}$; user terminal $P_tG_t = 5\,\text{dBw}$; axial ratio loss $L_a = 3\,\text{dB}$; noise figure $N_F = 3\,\text{dB}$; system noise temperature $T_s = 500\,\text{K}$. Additionally, according to [15], the typical standard deviation σ_s of PCE for shadowed user is $2\,\text{dB} \sim 4\,\text{dB}$, and the σ_{us} value of PCE for unshadowed user is $1\,\text{dB} \sim 2\,\text{dB}$. The required threshold $EINR_{req}$ is $5.5\,\text{dB}$.

4.2. Numerical Results

4.2.1. The Result of SAPSOIC Multibeam Pattern Synthesis Method

In Figures 5 and 6, 3-D gain pattern and contour in uv-coordinate of SAPSOIC synthesis are depicted, respectively. Compared with Figure 4, the gain is more focused in the required coverage area ($\pm 55°$) after SAPSOIC pattern synthesis, and the optimized pattern gain at the edge of beam coverage is
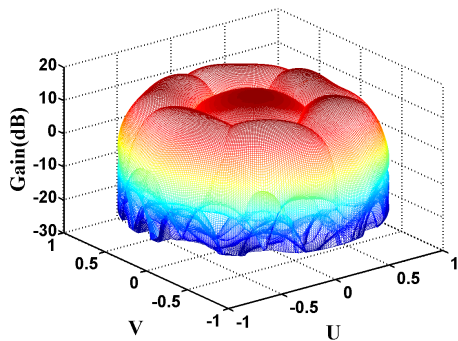
Figure 5. 3D seven-beam gain pattern of SAPSOIC synthesis.
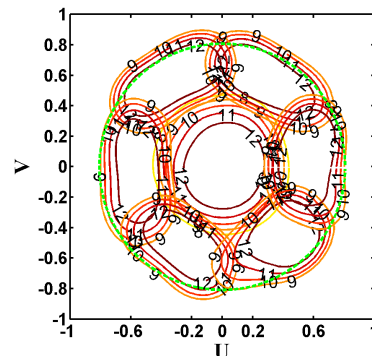
Figure 6. The contour of SAPSOIC-based synthesis seven-beam pattern.
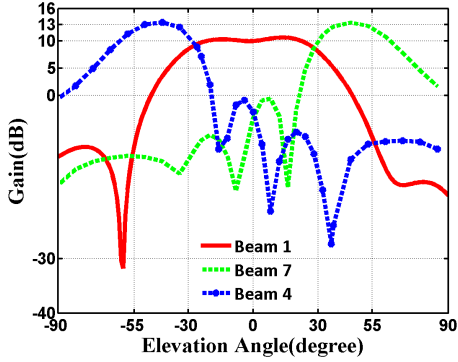
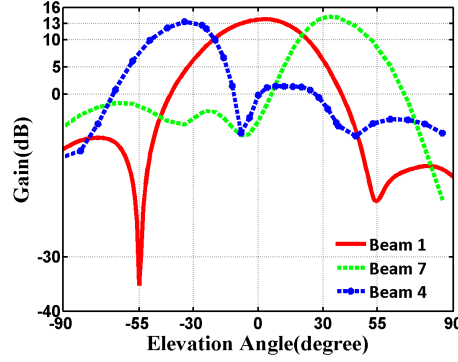**Figure 7.** The sectional gain patterns of the original three beams at $\varphi = 0°$.

Figure 8. The sectional gain patterns of the optimized three beams at $\varphi = 0°$.
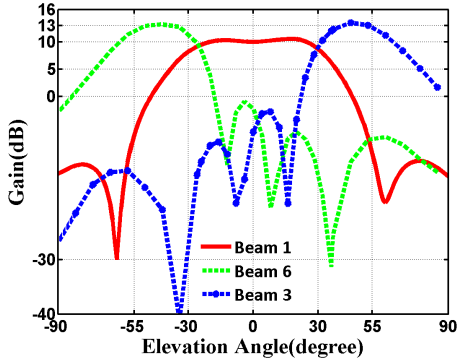

Figure 9. The sectional gain patterns of the original three beams at $\varphi = 120°$.
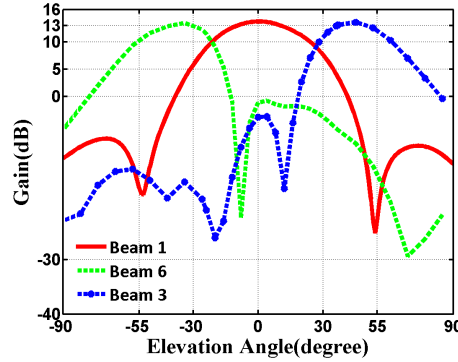

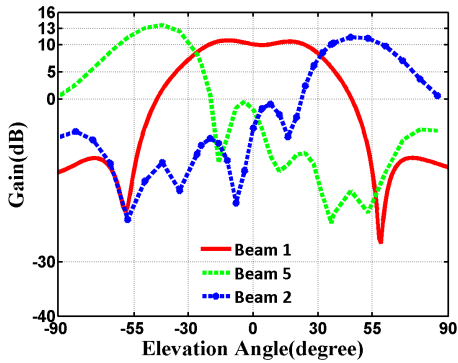**Figure 10.** The sectional gain patterns of the optimized three beams at $\varphi = 120°$.

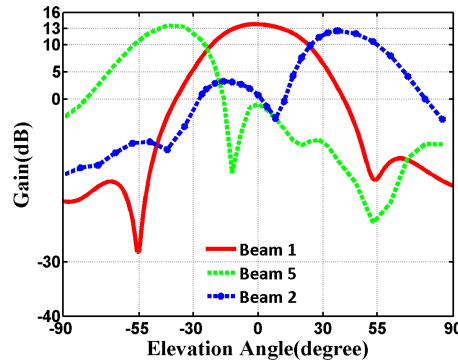**Figure 11.** The sectional gain patterns of the original three beams at $\varphi = 210°$.

Figure 12. The sectional gain patterns of the optimized three beams at $\varphi = 210°$.

decreased, but the gain in only a fraction of outskirts area is dropped to 9 dB. Moreover, the area where gain is greater than 12 dB is enlarged in center beam contour of Figure 6, and meanwhile, the beam gain is increased in overlap area (between center beam and outer six beams).

Figure 7 shows sectional gain patterns of beam 1, beam 4 and beam 7 at $\varphi = 0°$ before SAPSOIC synthesis optimization, and the optimized result is depicted in Figure 8. It is apparent that the first pattern null of optimized center beam moves to $-55°$ and $55°$, and the maximal main-lobe gain of center beam is increased by about 3 dB. Moreover, the roll-off of these three beams' main-lobe is much

steeper than non-optimized case. Both the optimized outer beam 4 (plotted as a dashed line with "∗" marker) and beam 7 (plotted as a dashed line) patterns have moving trends toward the middle. The sectional beam pattern comparisons among beam 1 and beam 3 and beam 6 at $\varphi = 120°$ are described in Figures 9 and 10, and Figures 11 and 12 illustrate the non-optimized and optimized sectional beam patterns of beam 1, beam 2 and beam 5 at $\varphi = 210°$ and give the same results.

According to the above comparison, it appears clearly that the optimized pattern achieves a "max-gain-flux" seven-beam coverage. Generally, the "iso-flux" beam coverage is a final objective pursued by many traditional pattern synthesis methods of space-borne multibeam antenna [19, 20], as depicted in Figure 7, where center-beam gain is less than outer six-beams gain. However, in terms of capacity increase, it is strongly suggested that "max-gain-flux" beam coverage has the competitive advantage over the "iso-flux" beam coverage in multibeam SatCom system using CDMA.

4.2.2. Capacity Analysis Result

Figures 13 and 14 compare the outage probability affected by PCE for unshadowed and shadowed users in two kinds of beam coverage, respectively. The values of PCE parameter, σ_s and σ_{us}, are 2.5 dB in Figure 13 and 1 dB in Figure 14. As shown in these two figures, user capacity is reduced obviously with σ_{us} or σ_s increases. Particularly, user capacity is improved more than one time higher in the "max-gain-flux" coverage synthesized by SAPSOIC than that of non-resynthesis "iso-flux" coverage. As shown in Figure 13, when $P_{out} = 10\%$, the user number per beam is only 5 at $\sigma_{us} = 1$ dB (depicted as solid line) and 7 at $\sigma_{us} = 0.5$ dB in the original seven-beam coverage; however, the user numbers per beam cell are nearly 11 and 15 in the same condition after SAPSOIC synthesis. In Figure 14, user capacity is about 3 when $P_{out} = 10\%$, $\sigma_s = 3.5$ dB in the non-resynthesis coverage, but capacity is increased to 8 in the synthesized "max-gain-flux" coverage.
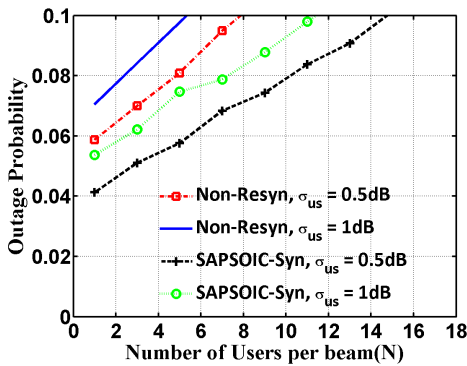
Figure 13. User capacity affected by δ_{us} and beam pattern ($\delta_s = 2.5$ dB, $EINR_{req} = 5.5$ dB).
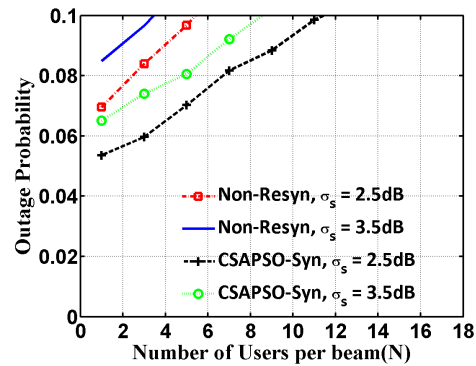
Figure 14. User capacity affected by δ_s and beam pattern ($\delta_{us} = 1$ dB, $EINR_{req} = 5.5$ dB).

5. DISCUSSION

According to the results of Section 4, user capacity is improved obviously under the "max-gain-flux" beam coverage; however, the quality of coverage in the outskirts area is degraded slightly, compared with the original seven-beam pattern. The decrease of gain at the edge of beam coverage is acceptable in LEO SatCom system, due to the high-speed moving of LEO satellite. It is assumed that the satellite moves in near-circular orbit, and the moving velocity v of this satellite is expressed as: $v = \sqrt{GM/(R_e + H)}$, where G is gravity constant, M the mass of earth, and R_e the radius of earth. So $v \approx 6.49$ km/s. The maximal spending time of one user from $\theta = 55°$ to $\theta = 54°$ is about 13 s, without considering earth rotation. The time in poor coverage is short, and the beam gain of user at the edge of coverage formerly can be improved quickly.

6. CONCLUSION

This paper uses a standard hexagonal array antenna combined with SA-based PSO to increase user capacity for CDMA-based SatCom system. We hunt an important relationship between user capacity and multibeam pattern, and propose a novel object function of array pattern synthesis, which is communication outage probability instead of the antenna metric function. The most interesting finding of this paper is that user capacity is doubled at least in the optimized beam coverage. For increasing capacity in the multibeam SatCom system using CDMA, the space-borne array pattern should have the following features: 1) the beam pattern needs to drop rapidly in the overlap area of multiple beam; 2) the "max-gain-flux" multibeam coverage can improve capacity compared with the traditional "iso-flux" coverage, at the expense of the gain decrease in some outskirts area. Although the degradation of coverage is acceptable, the multi-objective evolutionary algorithm (MOEA) is considered to seek a tradeoff between the quality of coverage and the maximal user capacity in the future.

REFERENCES

1. Rohwer, A. B., D. H. Desrosiers, W. Bach, et al., "Iridium main mission antennas: A phased array success story and mission update," *IEEE International Symposium on Phased Array Systems and Technology*, 504–511, 2010.
2. Croq, F., E. Vourch, M. Reynaud, et al., "The Globalstar 2 antenna sub-system," *3rd European Conference on Antennas and Propagation*, 598–602, 2009.
3. Johnson, J. M. and Y. Rahmat-Samii, "Genetic algorithm optimization and its application to antenna design," *Antennas and Propagation Society International Symposium*, Vol. 1, 326–329, 1994.
4. Liang, G., W. Gong, H. Liu, and J. Yu, "Development of 61-channel digital beam-forming (DBF) transmitter array for mobile satellite communication," *Progress In Electromagnetics Research*, Vol. 97, 175–195, 2009.
5. Liang, G., W. Gong, H. Liu, and J. Yu, "A semi-physical simulation system for DBF transmitter array on LEO satellite," *Progress In Electromagnetics Research*, Vol. 97, 197–215, 2009.
6. Recioui, A., " Sidelobe level reduction in linear array pattern synthesis using particle swarm optimization," *Journal of Optimization Theory and Applications*, Vol. 153, No. 2, 497–512, 2012.
7. Li, X. and M. Yin, "Hybrid differential evolution with artificial bee colony and its application for design of a reconfigurable antenna array with discrete phase shifters," *IET Microwaves Antennas & Progapation*, Vol. 6, No. 14, 497–512, 2012.
8. Wang, F., V. Balakrishnan, P. Y. Zhou, et al., "Optimal array pattern synthesis using semidefinite programming," *IEEE Transactions on Signal Processing*, Vol. 51, No. 5, 1172–1183, 2003.
9. Fuchs, B., A. Skrivervik, and J. R. Mosig, "Shaped beam synthesis of arrays via sequential convex optimizations," *IEEE Antennas and Wireless Propagation Letters*, Vol. 12, 1049–1052, 2013.
10. Gilhousen, K. S., I. M. Jacobs, et al., "Increased capacity using CDMA for mobile satellite communication," *IEEE Journal on Selected Areas in Communications*, Vol. 8, No. 4, 503–514, 1990.
11. Fu, H., G. Bi, and K. Arichandran, "Capacity comparison of CDMA and FDMA/TDMA for a LEO satellite system," *IEEE International Conference on Communication*, 1069–1073, 1999.
12. Fu, H., G. Bi, and K. Arichandran, "Performance of multibeam CDMA-based LEO satellite systems with imperfect power control," *International Journal of Satellite Communications*, Vol. 16, No. 3, 155–167, 1998.

13. Song, H., G. Liang, W. Gong, et al., "Performance analysis of a seven-beam CDMA-based LEO satellite system," *IEEE Asia-Pacific Conference on Antennas and Propagation*, 174–175, 2012.

14. Microwave Vision Group, *Antenna Measurement and Radome Test System*, MVG-EBOOK, 2013.

15. Monk, A. M. and L. B. Milstein, "Open-loop power control error in a land mobile satellite system," *IEEE Journal on Selected Areas in Communications*, Vol. 13, No. 2, 205–212, 1995.

16. Clerc, M. and J. Kennedy, "The particle swarm — Explosion, stability, and convergence in a multidimensional complex space," *IEEE Transactions on Evolutionary Computation*, Vol. 6, No. 1, 58–73, 2002.

17. Cardone, G., G. Cincotti, and M. Pappalardo, "Design of wide-band arrays for low side-lobe level beam patterns by simulated annealing," *IEEE Transactions on Ultrasonics, Ferroelectrics, and Frequency Control*, Vol. 49, No. 8, 1050–1059, 2002.

18. Lutz, E., D. Cygan, M. Dippold, et al., "The land mobile satellite communication channel — Recording, statistics, and channel model," *IEEE Transactions on Vehicular Technology*, Vol. 40, No. 2, 375–386, 1991.

19. Liang, G., B. Jia, W. Gong, et al., "Design of phased array antenna on satellite with iso-flux beam coverage," *Chinese Journal of Radio Science*, Vol. 25, No. 2, 248–252, 2010.

20. Jin, J., H. Wang, M. Liu, et al., "Genetic algorithms based isoflux multi-beams optimization for non-GEO satellites," *Proceedings of The International Conference Information Computing and Automation*, Vol. 1, No. 3, 1274–1277, 2008.